OVERVIEW OF ^{14}C RELEASE FROM IRRADIATED ZIRCALOYS IN GEOLOGICAL DISPOSAL CONDITIONS

S Necib[1]* • C Bucur[2] • S Caes[3] • F Cochin[4] • B Z Cvetković[5] • M Fulger[2] • J M Gras[1] •
M Herm[6] • L Kasprzak[7] • S Legand[7] • V Metz[6] • S Perrin[8] • T Sakuragi[9] • T Suzuki-Muresan[10]

[1]Andra, Meuse, Haute-Marne Center, RD960, 55290 Bure, France.
[2]RATEN ICN, Institute for Nuclear Research Campului 1, Mioveni, 115400, Romania.
[3]SCK·CEN, Herrmann-Debroux 40, 1160 Brussels, Belgium.
[4]AREVA, Tour Areva -1, place Jean Millier, 92084 Paris La Défense cedex, France.
[5]PSI, Labor für Endlagersicherheit, OHLD/111, CH-5232 Villigen PSI, Switzerland.
[6]KIT, Hermann-von-Helmholtz-Platz 1, 76344 Eggenstein-Leopoldshafen, Germany.
[7]CEA – Service d'Etudes Analytiques et de Réactivité des Surfaces (SEARS), CEA, Université Paris-Saclay, F-91191
 Gif sur Yvette, France.
[8]CEA – Service d'Etude et Comportement des Matériaux de Conditionnement (SECM), CEA, F-30207 Bagnols-
 sur-Cèze, France.
[9]RWMC, 1-15-7 Tsukishima Chuo-ku, Tokyo 104-0052, Japan.
[10]Armines, 60 Boulevard Saint-Michel, 75272 Paris, France.

ABSTRACT. Carbon-14 (radiocarbon, ^{14}C) is a long-lived radionuclide (5730 yr) of interest regarding the safety for
the management of intermediate level wastes (ILW). The present study gives an overview of the release of ^{14}C from
irradiated Zircaloy cladding in alkaline media. [14]C is found either in the alloy part of Zircaloy cladding due to the
neutron activation of ^{14}N impurities by $^{14}N(n,p)^{14}C$ reaction, or in the oxide layer (ZrO_2) formed at the metal surface
by the neutron activation of [17]O from UO_2 or $(U-Pu)O_2$ fuel and water from the primary circuit in the reactor by [17]O
$(n,\alpha)^{14}C$ reaction. Various irradiated and unirradiated Zircaloys have been studied. The total ^{14}C inventory has been
determined both experimentally and by calculations. The results seem to be in good agreement. Leaching experiments
were conducted in alkaline media for several time durations. [14]C was mainly released as carboxylic acids. Further,
corrosion measurements were performed by using both hydrogen measurements and electrochemical measurements.
The corrosion rate (CR) ranges from a few nm/yr to 100 nm/yr depending on the surface conditions and the method
used for measurement. From a safety assessment point of view, the instant release fraction (IRF) was determined on
irradiated Zircaloy-2. The results showed that the ^{14}C inventory in the oxide was significantly below the 20% com-
monly used in safety case assessments.

KEYWORDS: activated Zircaloy, alkaline media, corrosion, ^{14}C speciation, geological disposal.

INTRODUCTION

Zirconium alloys are used as cladding materials surrounding the fuel in light water reactors. After being unloaded from the reactor, they can be disposed of as spent fuel or reprocessed before their disposal in a geological repository. At the reprocessing facility, the spent fuel assemblies are first stored in the deactivation pool for a few years (1–4), and then they are sheared in hulls and end-pieces, in order to dissolve the fuel pellets in boiling concentrated nitric acid. In principle, these steps do not affect the retention of the zirconia layers or the corrosion resistance of the hulls (Gras 2014).

In zirconium alloy claddings, the neutron activation of ^{14}N, on impurity element of these alloys, is the main source of carbon-14 (radiocarbon, ^{14}C). [17]O coming from the UO_2 (or $(U-Pu)O_2$) oxide fuel and from water coolant is also a significant precursor of ^{14}C in the zirconium oxide layers formed in reactor on the internal and external sides of cladding respectively. The actual

*Corresponding author. Email: sophia.necib@andra.fr.

nitrogen content of zirconium alloys is in the order of 40 ppm, so two times lower than the maximum level of 80 ppm set as specified values.

Prior to the CAST[1] project, inventories of ^{14}C in hulls were mainly determined by calculation. The ^{14}C specific activity in cladding was estimated around $1–5 \times 10^4$ Bq.g^{-1}. The inventories have often been overestimated, based on higher nitrogen content than in reality.

In the literature, there is a lack of reliable data on the chemical state of ^{14}C in the metal and in zirconium oxide layer. According to Yamaguchi (1999) and Yamashita (2013), the measured ^{14}C specific concentrations in zirconia oxide layers are about twice that of Zircaloy metal after irradiation in a reactor.

The mechanisms and rate of ^{14}C release from hulls were assumed to be controlled in large part by the uniform corrosion rate of Zircaloy at low or moderate temperature, the diffusion rate of ^{14}C from zirconia oxide layers and/or the dissolution rate of zirconia oxide layers, at the time of the contact between hulls and the infiltrated water under repository conditions. Nevertheless, various questions arose regarding the physical conditions of these hulls, i.e., their state of division and fragmentation. Indeed, the bulk Zircaloy of hulls is hydrided in reactor, linked to the burn-up, which makes the metal brittle and probably more or less fragmented if it is press-compacted during waste processing.

From the literature, the uniform corrosion rates of zirconium alloys are very low in anaerobic neutral or alkaline waters at low temperature with an upper value of 20 nm.yr^{-1} (Kato 2013).

Study of the corrosion behavior of Zircaloy in high temperature water showed that, when the zirconia oxide layer reaches a critical thickness of ~ 2.5 μm (corresponding to a weight gain of 30–40 mg.dm^{-2}), there is a change in the corrosion regime: the corrosion kinetics first follow a power law (a priori a cubic law) and after the break-away point pseudo-linear kinetics apply.

The zirconia oxide layer formed on spent fuel rod cladding is chemically very stable in pure water (a solubility of 10^{-9} M can be considered as a conservative and realistic estimate). The solubility increases with increasing alkaline concentrations, and reaches values in the order of 10^{-6} M at pH 12.5 at ambient temperature. The zirconia solubility remains very low for carbonate concentrations lower than 10^{-2} M. At low to moderate concentrations, chloride ions do not seem to have any significant effect on the zirconia solubility, except in CaCl$_2$ solutions of concentration higher than 0.05 M at pH > 10 due to the formation of a highly soluble complex with calcium.

A lack of knowledge of whether the release of radionuclides can be considered as congruent with the dissolution of zirconia led to the conservative assumption in performance assessment studies that the oxide layer provides no delay to the release of radionuclides. Previous studies revealed that both organic and inorganic carbons were identified in leaching experiments with irradiated hulls or non-activated Zr-based materials (Zr and ZrC powders), although a higher proportion was clearly released as small organic molecules.

The aim of this paper is to give an overview of the ^{14}C inventory in Zircaloys (spent fuel and hulls) as well as its release in terms of quantification and speciation, in alkaline media at room

---

[1]The CAST (CArbon-14 Source Term) project aimed to develop a better understanding of the potential release mechanisms of carbon-14 from radioactive waste materials under conditions relevant to waste packaging and disposal to underground geological disposal facilities.

temperature. To achieve these objectives, ^{14}C inventory was determined experimentally by means of digestion experiment as well as by calculations. In addition, leaching experiments were conducted in NaOH and Ca(OH)$_2$ solutions on various types of Zircaloys for different time durations to measure released ^{14}C concentrations in solution as well as to identify the speciation. Corrosion rate measurements were carried out to study the release mechanism and investigate the potential relationship between metal dissolution and ^{14}C release.

MATERIALS

Unirradiated Zirconium, Zircaloy-2 (Zr-2) and Zircaloy-4 (Zr-4) were investigated as well as irradiated Zircaloy-2, Zircaloy-4 and M5^{TM}. Unirradiated samples were plates or tubes while irradiated samples were hulls or rings directly machined from the claddings subjected to burnups ranging from 7.5 to 60 GWd/tHM. The nitrogen concentration was in the range of 17–34 ppm for as received Zr-2 and Zr-4. Unirradiated materials were in the as-received or preoxidized conditions in order to form an oxide layer up to 2.7 μm thick. Unirradiated samples were cleaned with ethanol. Zircaloy ring samples cut from spent fuel rods (which contains other radioelements) were rinsed with HNO$_3$, followed by rinsing with water and air drying, and irradiated materials other than spent fuel, were simply rinsed with water and air dried.

METHODS

Materials Characterization

Metallography was carried out to identify the microstructure of the metal and zirconia layers. Scanning electron microscopy (SEM) as well as transmission electron microscopy (TEM) observations were carried out.

Leaching Experiments

In order to determine the ^{14}C release from irradiated Zircaloys, leaching experiments were conducted in alkaline media (NaOH or Ca(OH)$_2$ solutions, pH 12) at room temperature under anaerobic conditions for various time durations ranging from 14 days to 6.5 years. The solutions were specifically chosen to simulate repository conditions representative of the disposal of intermediate-level long lived wastes.

Corrosion Rate Measurements

Various corrosion rate measurements were made on both irradiated and unirradiated Zr alloys in anoxic alkaline conditions at room temperature. The corrosion rates were determined using both electrochemical techniques and based on the amount of either evolved H$_2$ or released ^{14}C. Electrochemical measurements involved the linear polarization technique consisting of polarizing an electrode made of Zircaloy around the free corrosion potential Ecorr (± 10 mV or ± 25 mV) to determine the polarization resistance and therefore the corrosion rate. To do so, a potentiostat/galvanostat AUTOLAB 302, with NOVA 1.11 corrosion software was connected to a glass cell (90 mL) equipped with a five hole lid: four holes for the Ag/AgCl reference electrode, the Pt counter electrodes, and the working electrode, and a hole for the bubbling tube. After the electrodes were mounted, the vessel lid was made tight using resin or glue.

All electrodes and the bubbling tube were immersed into 30 mL NaOH 0.01M solution (pH = 12 and conductivity of 2.1 mS/cm). Before starting each experiment, the device was calibrated using an AUTOLAB Dummy Cell 2 and nitrogen gas was bubbled into solution for

2 hours prior to running the electrochemical test as well as during the test. The electrochemical assembly was mounted into a Faraday cage to avoid electromagnetic interferences from external sources.

Initially, the working electrode (a 2.5 cm^2 Zr sample) was immersed in solution and kept for 10 min to stabilize at the free corrosion potential Ecorr.

The applied potentials were ±10 mV and ±25 mV vs Ecorr using a scan rate of 0.16 mV/sec. The polarizing potentials were sufficiently low to avoid disruption of the oxide layer. Following polarization, the Tafel plots were generated using NOVA 1.11 software and corrosion rates were computed (ASTM G 102, 2004).

The Faraday's law was used to calculate the corrosion rate (CR) and mass loss rate (MR) as expressed in Equations (1) and (2):

$$CR = K_1 * (icorr / \rho) * EW \tag{1}$$

$$MR = K_2 * icorr * EW \tag{2}$$

where CR is the corrosion rate, mm/yr; MR is the mass loss rate, mg/dm^{2}d (mdd); ρ is the Zr density, g/cm^3; icorr is the corrosion current density, µA/cm^2; EW is the equivalent weight (dimensionless—for Zr EW = 23); K_1 and K_2 are constants (K_1 = 3.27E-03 mm × g/µA/ cm/yr and K_2 = 0.0895 g × cm^2/µA/dm^2/d).

Hydrogen measurements were used to determine the corrosion rate on unirradiated Zircaloys based on Equation (3). The corrosion rate for unirradiated Zr alloys can be obtained from the total amount of generated hydrogen (gas and absorbed).

$$Zr + 2H_2O \rightarrow ZrO_2 + 2H_2 \tag{3}$$

The corrosion rate for irradiated Zircaloy-2 was obtained from the released ^{14}C fraction, using Zr-2 cladding free from oxide film, immersed in a dilute NaOH solution of pH 12.5 and nitrogen atmosphere at room temperature around 293 K. Assuming that the activated ^{14}C is distributed homogeneously in the cladding and that it is released congruently with corrosion of the alloy, the equivalent corrosion rate, R_{eq}, can be obtained from Equation (4):

$$R_{eq} = \frac{aL}{2At} \tag{4}$$

where a is the leached amount of ^{14}C (Bq), A is the inventory in the cladding (Bq), L is the thickness of the cladding (nm), and t is the test time (yr).

^{14}C Measurements

Inventory Measurements

^{14}C inventory was measured experimentally as well as by modeling. Digestion experiment in (16% H$_2$SO$_4$ + 3% HF) solution was carried out to determine experimentally the inventory on spent fuel Zr-4 exposed to a burn up of 50.4 GWd/tHM. In addition, it was determined on Zr-4 hulls in 20% HNO$_3$ and diluted fluoric acid (6%HF). The activation of the fuel rod segment was calculated using two independent approaches: (1) the neutron flux of the subassembly was simulated using the Monte Carlo N-particle code (MCNP) and finally the CINDER program calculated the activation of the material (Wilson 2008; Pelowitz 2011); and (2) the SCALE/ TRITON package was used to develop cladding macro-cross-section libraries, which were used

in the ORIGEN-S program to calculate the radioactive inventory of the cladding (Gauld 2009; ORNL 2011).

Speciation and Quantification

Inorganic and organic fractions were measured on Zircaloy-2, Zircaloy-4, and M5™. To separate the organic and inorganic fractions, acid dissolution was carried out followed by wet oxidation (Magnusson 2008). ^{14}C speciation was determined by using anion, ion chromatography and gas chromatography. ^{14}C was quantified by using liquid scintillation counting (LSC) and accelerated mass spectroscopy (AMS).

RESULTS AND DISCUSSION

Material Characterizations

Observations on unirradiated Zircaloys revealed intermetallic Laves phases as shown in Figure 1. In the preoxidized conditions, the oxide layer was uniformly formed at the metal surface and hydrides formed in the metal as shown in Figure 2. Figures 3–5 show some examples of characterizations carried out on irradiated Zircaloys. Figure 3 shows the oxide layer along an irradiated Zr-4 cladding as well as the hydrides. Figure 4 presents the ring samples taken from a Zr-2 cladding as well as a cross section revealing the oxide thickness. Figure 5 presents micrographs of radiation induced defects on an irradiated Zr-4.

^{14}C Measurements

^{14}C Inventory

Analysis of the ^{14}C inventory in Zircaloy claddings was carried out by calculation as well as experimentally. According to the specified or measured N content of unirradiated Zircaloy-4, the calculated ^{14}C inventory was estimated between 1.7 and 3.5×10^4 Bq/g. Experimental measurements revealed values of the same order of magnitude (see Table 1). The N content
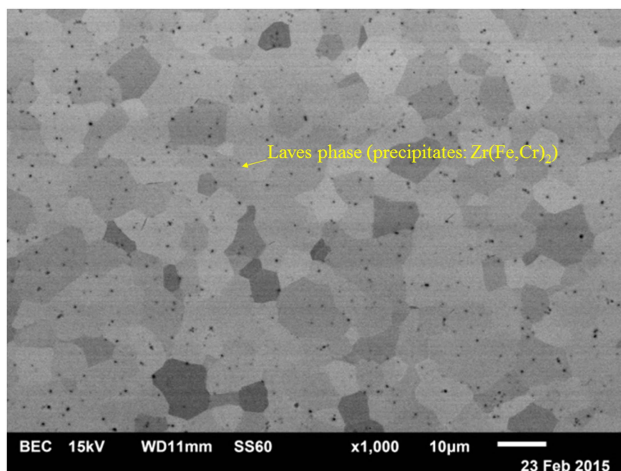

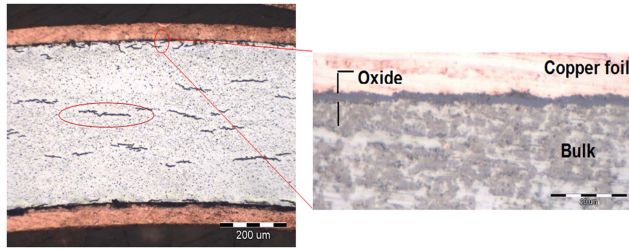Figure 1 Scanning electron microscopy (BSE mode) of an unirradiated Zr-4.

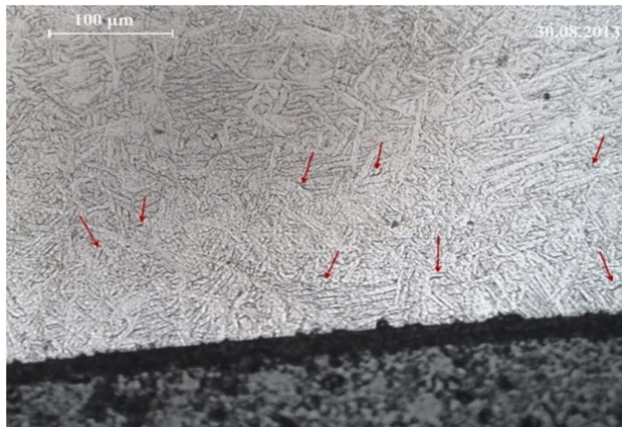Figure 2 Preoxidized unirradiated Zr-4 (oxide thickness = 2.7 μm).

Figure 3 Transmission electron microscopy of an irradiated Zr-4: outside oxide layer along the spent fuel cladding. The red arrows indicate the presence of hydrides.
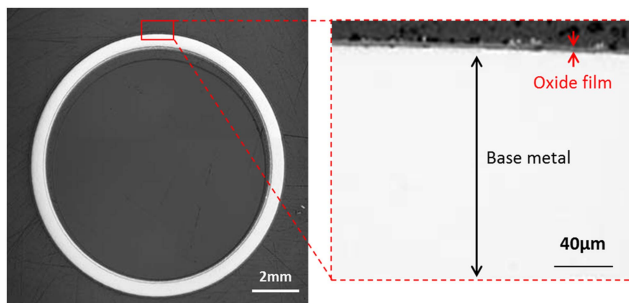

Figure 4 Scanning electron microscopy of an irradiated Zr-2 (BWR STEP III) ring sample (from cladding) before testing, oxide thickness = 2.7 μm. (Left) Cross section of the cladding showing the metal and oxide; (right) higher magnification of the oxide area.

determined experimentally on Zircaloy-4 was significantly below the specified value (~20 ppm vs. 80 ppm), which directly impacted the ^{14}C inventory in cladding material and allowed more accuracy of the calculations.
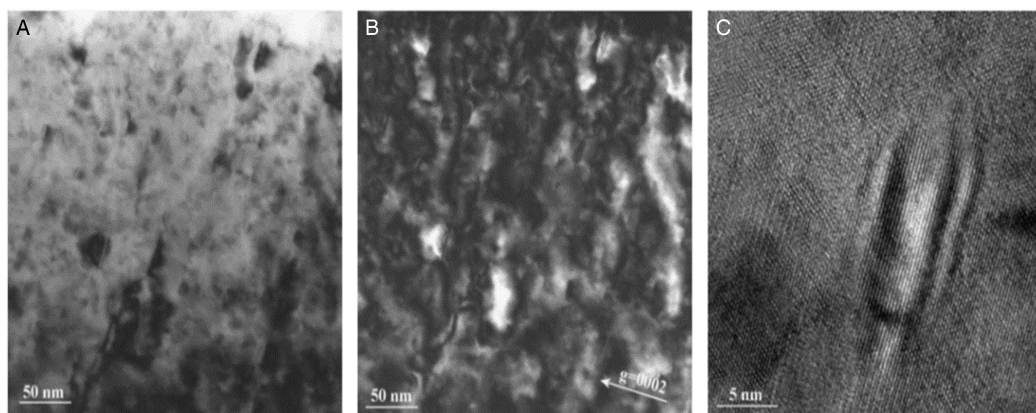
Figure 5   Micrographs of the radiation induced defects in the cladding of Zr-4: (A) bright field, (B) dark field, (C) high-resolution micrograph of a radiation induced dislocation loop.

Table 1 ^{14}C inventory (modeling and experimental results).

| Zircaloy type	N content (ppm)	Burnups GWd/ThU	Inventory modeling (Bq/g)	Inventory experiments (Bq/g)
Zr-4	50 (specified)	50.4	$3.5 \pm 0.4 \times 10^4$	$3.7 \pm 0.4 \times 10^4$
Zr-4 (CANDU)	30 (specified)	7.5	1.78×10^4	$2.12 \pm 0.3 \times 10^4$
Zr-4	17–25 (experimentally determined)	60	$1.3–1.9 \times 10^4$	
Zr-2	NA	34–41		$1.5–3.5 \times 10^4$
Zr-2 metal				2.5×10^4
Zr-2 outer oxide				5×10^4
Zr-4	34 (specified)	54.50	1.78×10^4	
M5^{TM}	27(specified)	46.57	3.03×10^4	

^{14}C Speciation and Quantification

The measurements of ^{14}C were very challenging and required the development of highly sensitive techniques well adapted to measure very low ^{14}C concentrations. The LSC technique was widely used to determine the inorganic/organic partition. However this technique presented some limits when it came to quantification of given collected fractions. The ^{14}C inorganic/organic partition was measured on M5^{TM}, Zr-4 (CANDU) and Zr-4 for various times (see Table 2).

The results show that both inorganic and organic molecules were released in alkaline solution. The Zircaloy type seems to influence the inorganic/organic partition as shown with the M5^{TM} and Zr-4 exposed to the same conditions for 14 days and 6 months. The speciation did not vary between 14 days and 6 months. Long time exposure revealed a majority of organic molecules released in alkaline media. Additional work carried out on hulls free from oxide showed an evolution of the ^{14}C speciation over time (see Figure 6). Below one year, ^{14}C was mainly

Table 2 ^{14}C inorganic/organic partition measured between 14 days and 6.5 years.

Zircaloy type	Inorganic(%)	Organic(%)	Gas	Leaching time
M5^{TM}	55	45	ND	14 days and 6 months
Zr-4	80	20		
CANDU-Zr-4	40	60	ND	18 days, 6 months, 8 months, 10 months, 12 months and 18 months
Zr-2	20.6	63.3	16.2	6.5 years

ND = not detected.
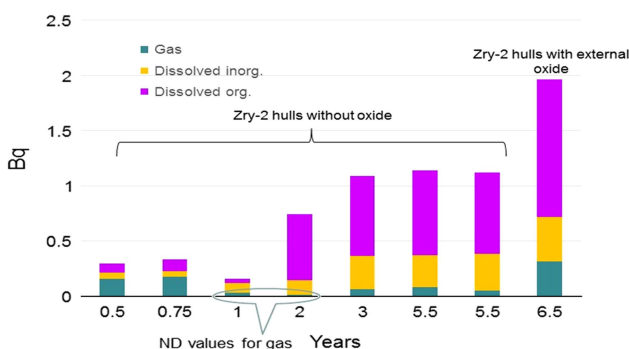
Figure 6 ^{14}C measured on irradiated Zircaloy-2 (metal + oxide) and Zircaloy-2 (metal only).

Table 3 ^{14}C speciation in alkaline media (NaOH or Ca(OH)$_2$ solutions).

| Zircaloy type | ^{14}C speciation | | | | Method |
	Solutions	Organics	Inorganics	Gas	
Zr-4 + M5^{TM}	NaOH	Glycolate Acetate Formate Oxalate	Carbonate		Anionic chromatography
	Blank	Acetate Formate	Carbonate		Anionic chromatography
Zr-4	Ca(OH)$_2$	Acetate Formate		Methane Ethene CO$_2$	Ion chromatography Gas chromatography
Zr-4 + M5^{TM}	NaOH	Formate Acetate Propionate Oxalate			Ion chromatography

released as gas while from two years, ^{14}C releases were about 27% of dissolved inorganic compounds, 66% of organic compounds and the remaining as gas. Organic compounds were analysed in more detail (see Table 3) to determine the speciation in alkaline media. Carboxylic acids such as glycolate, acetate, formate, oxalate and propionate were identified on Zr-4 and M5^{TM} hulls. Methane, ethene and CO$_2$ were detected in the gas phase. Contamination cannot

Table 4 ^{14}C quantification of the inorganic and organic fractions.

Media	Duration	Materials	Organic (Bq/g)	Inorganic (Bq/g)	Method
NaOH	14 days and 6 months	M5^{TM}	101 ± 10	110 ± 10	LSC
NaOH	From 18 days to 18 months	Zr-4 (CANDU)	7 ± 1.0	4.0 ± 1.0	LSC
NaOH	5.5 years	Zr-2 (metal + oxide)	0.49		LSC
		Metal	0.14		
NaOH	6 months	M5^{TM}	179 (Formate)	—	LSC
			71 (Acetate)		
			65 (Propionate)		
			19 (Oxalate)		
	6 months	M5^{TM}	9 (Oxalate)	—	AMS

be excluded as measurements on the blank test (NaOH solution only) highlighted the presence of acetate and formate as well. The AMS confirmed the presence of organic molecules such as oxalate, identified by ion chromatography (IC).

The results obtained on the M5^{TM} hull leached for 6 months in NaOH solution highlight the discrepancy from one technique to another. Indeed, the determined ^{14}C specific activity was ranging from 100 to 300 Bq/g depending on the applied procedure (see Table 4).

Analyses were also conducted on the oxalate molecule in order to determine the specific activity of ^{14}C by using the LSC technique as well as the AMS. The results for the M5^{TM} hulls leached for 6 months in NaOH solution, showed a specific activity of 19 Bq/g hulls and 9 Bq/g hulls respectively, with the LSC and AMS measurements highlighting the inaccuracy of the measurements. At this stage, the quantification needs more work to provide a thorough understanding. Indeed, the quantification obtained by the AMS and LSC techniques was very different and sometimes by several orders of magnitude. It is assumed that the AMS was more accurate due to its low detection limit. Overall, high risk of contamination and memory effect from previous analyses must be considered in the results. From the literature (Wieland 2010; Gras 2014), the aqueous C-H-O system in complete thermodynamic redox equilibrium would be dominated by carbonate and methane. Inorganics were also detected at lower concentrations according to the LSC measurements. The results obtained from the leaching experiments, conducted up to 6.5 years, revealed an evolution of the speciation with time; this affects the certainty of any long term predictions relevant to repository conditions. A fast release was confirmed in the early stage of leaching in alkaline media, followed by an extremely low rate afterwards.

Leaching and Corrosion Rate Measurements

In repository conditions, the instant release fraction (IRF) is of great interest from a safety assessment point of view. It is generally said that the IRF for ^{14}C is concentrated in the external oxide layer and estimated at 20% maximum of the total ^{14}C concentration. More recently, the IRF was estimated below 10% assuming a congruent release rate with a uniform corrosion rate of the metal. The results were obtained from irradiated Zr-2 (Sakuragi 2018). Regarding ^{14}C in the oxide as an IRF would be overly conservative, because the total amount of leached ^{14}C from the hull (metal + oxide) corresponds to 0.0038% of the total inventory after 6.5 years of immersion as mentioned before (Sakuragi 2018). Both the low amount of

^{14}C in the oxide and the low leaching rate indicate that ^{14}C in the oxide does not have a major impact on the IRF. This understanding should be reflected in the safety case. Other mechanisms need to be taken into consideration to explain the ^{14}C release from the oxide and metal.

In order to confirm or not a congruent ^{14}C release rate with the corrosion rate, measurements were carried out to determine the CR. Figure 7 shows the results for the CR of unirradiated Zircaloys immersed in NaOH solution at 25°C. For comparison, the results obtained in pure water and cementitious water are also plotted as significant work was previously carried out. In pure water, the zirconium alloys exhibit excellent corrosion resistance. This overview confirms low corrosion rates at low temperature (20°C) in NaOH solution for Zr-2 and Zr-4 by using hydrogen release measurements from unirradiated materials. The results confirmed that the Zircaloy type does not influence the corrosion rate. The corrosion rate decreases with time. It is slightly higher in artificial cementitious water than in pure water and NaOH solution. The chemical composition of the artificial cementitious water is given in Table 5. The chemical composition was calculated based on groundwater originating from the sea in equilibrium with Portland cement. This suggests that species such as chloride ion influence the corrosion kinetics. pH, temperature and time had already been pointed out as key parameters influencing the corrosion rates.

Figure 8 presents the results obtained in CAST for the CR of both unirradiated and irradiated Zircaloys.

The results obtained at low temperature by hydrogen measurements were consistent with previous work performed by (Kato 2013). Most of the experiments were conducted on as-received unirradiated Zircaloy, which means that the available results concerned the pre-transition regime (cubic law) only, with an oxide thickness $<< 2.5\ \mu m$. This overview includes the work
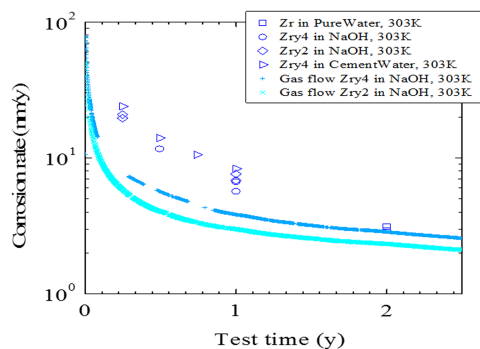

Figure 7　Corrosion rate of unirradiated Zr alloys versus time at 303 K.

Table 5　Chemical composition of groundwater in equilibrium with Portland cement (mol/L).

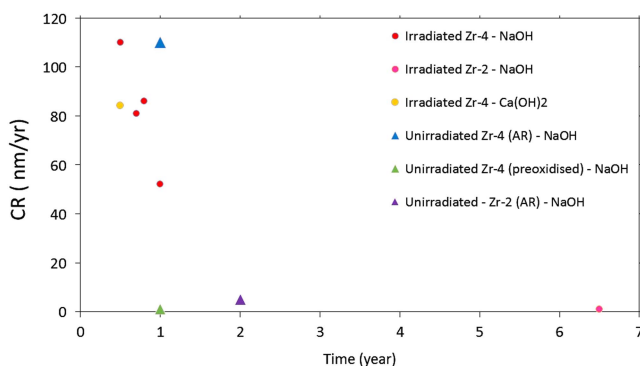| pH	Na$^+$	Cl$^-$	Ca^{2+}	SiO$_2$	Al^{3+}	SO$_4^{2-}$	Carbonate (HCO$_3^-$/CO$_3^{2-}$)
12.5	0.6	0.6	0.028	3.10^{-5}	$4.4.10^{-6}$	$2.4.10^{-4}$	$1.4.10^{-5}$

Figure 8 CR of unirradiated Zircaloys (Zr-4 in the as-received conditions) in NaOH solution (blue triangle), Zr-4 in the preoxidized conditions in NaOH solution (green triangle), Zr-2 in the as-received conditions (purple triangle) and irradiated Zircaloys (Zr-4 in NaOH solution (red circle), Zr-2 in NaOH solution (pink circle), Zr-4 in Ca(OH)$_2$ solution (yellow circle).

obtained on unirradiated preoxidized Zr-4 to explore the post-transition regime as well (Bucur et al. 2017). The corrosion rates were determined by applying linear polarization measurements on both as-received and preoxidized Zr-4 (oxide thickness ~2.7 μm) in NaOH solution, pH 12.5. The results were obtained for shorter times than those obtained by hydrogen measurements on Zr-2 and Zr-4 and the obtained values were higher (up to 100 nm/yr). The use of various techniques such as hydrogen measurements or linear polarization resistance (LPR) measurements for unirradiated materials and the released fraction of ^{14}C for irradiated Zircaloy makes it difficult to compare the results at short terms. The calculation of the corrosion rate based on a congruent release of ^{14}C with the metal loss has not been verified yet. It is known that electrochemical measurements are not sufficiently sensitive to measure very low corrosion rates.

Overall, the results support the change of kinetics as the oxide grows as preoxidized Zr exhibits a lower CR than the as-received one. Further data would help determine more accurately the applied law for the post-transition regime at low temperature.

The low corrosion rate of Zircaloy in alkaline environments at low temperature was confirmed, with similar values in NaOH and Ca(OH)$_2$ solutions. The influence of irradiation on the corrosion rate is not fully understood. Indeed, some results show a detrimental irradiation effect on the CR when comparing the preoxidized Zr-2 with the irradiated Zr-2 after 1 year in NaOH solution (Figure 8), while lower CR was measured for irradiated Zr-2 in comparison with unirradiated Zr-2 (see Figure 9). However, these results were obtained at higher temperature for unirradiated Zr-2, which thermally activated the corrosion processes. Figure 9 highlights that, by extrapolating at 80°C the data obtained by using the Hillner equation (suitable for high temperature conditions), the resulting CR is lower than the one measured experimentally. This suggests different corrosion processes between high and low temperatures (Sakuragi 2018). The influence of temperature on the corrosion kinetics is clearly demonstrated.

At high temperatures up to 350°C, Zircaloy exhibits excellent corrosion resistance thanks to the formation of the protective oxide film of ZrO$_2$. The existence of various models developed to account for the kinetics of uniform corrosion of Zircaloy-2 and -4 in high temperature water between 250 and 400°C was mentioned in the literature (Garzarolli 1980; Cox 1985; Gras 1988;
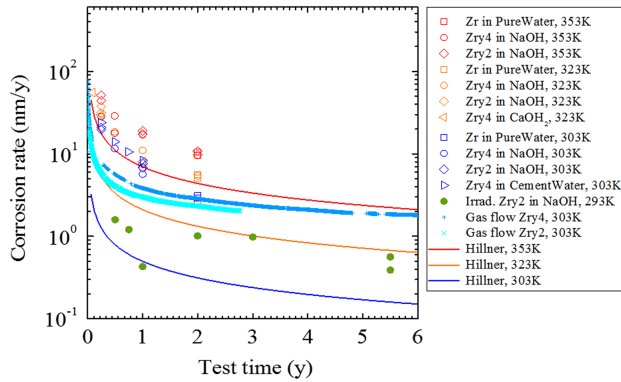
Figure 9   Corrosion rate for the unirradiated Zr alloys by the glass ampoule method under various conditions. As well as by using the gas flow system (SAK 2013), the equivalent corrosion rate for irradiated Zircaloy-2 (BWR cladding without oxide) obtained from leached ^{14}C, and the corrosion rate obtained from the Hillner equation (Hillner 1977) at any temperatures.
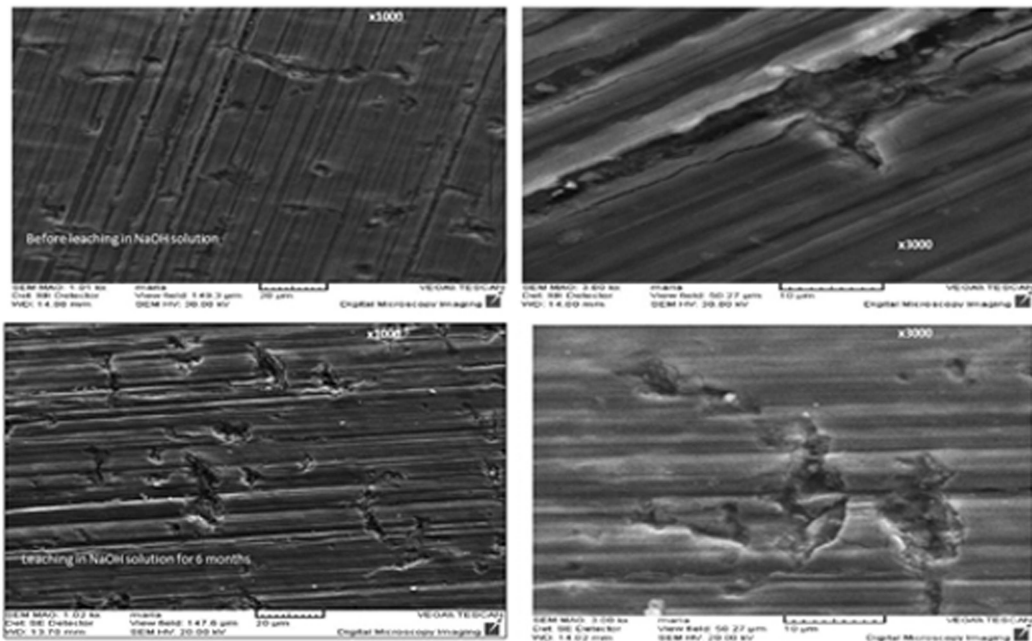

Figure 10   SEM images on irradiated Zr-4 samples: before leaching in NaOH solution (upper figures) and after leaching in NaOH solution for 6 months (lower figures).

IAEA 1998; Tanabe 2013). The models are semi-empirical models with a cubic rate law for the pre-transition period and a linear post-transition kinetic regime. It is known that the corrosion of zirconium is highly textured, probably because of the stress generated by the oxidation swelling. The grains organize themselves so that stress is minimized. Therefore, the surfaces are mainly the (-111) crystallographic plane, which is the most stable surface index.
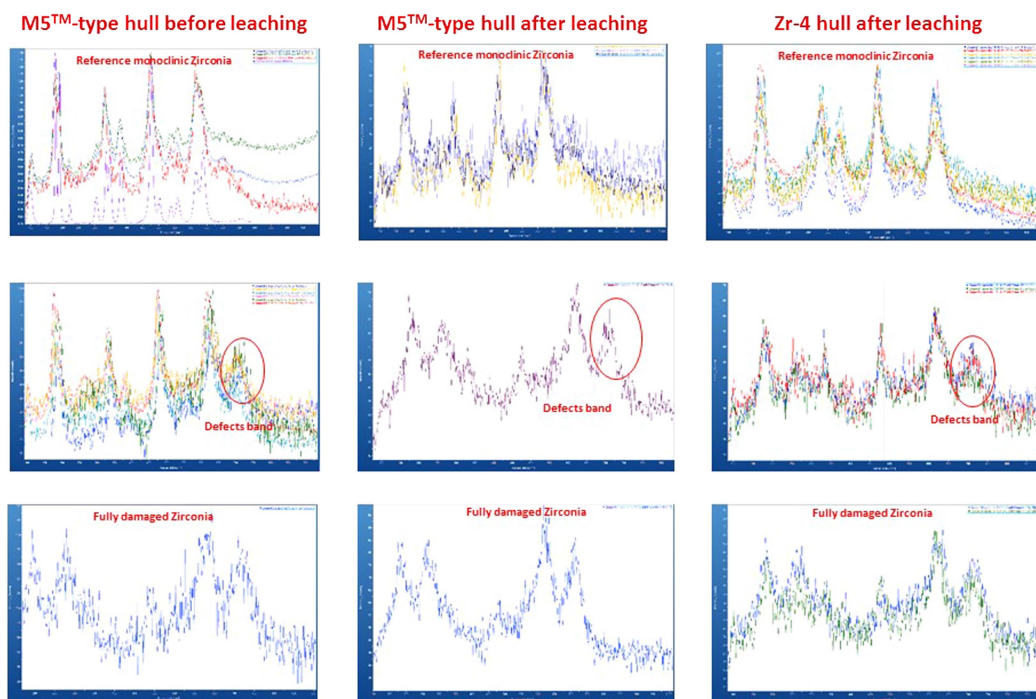
Figure 11 Raman spectra obtained on M5^{TM} and Zr-4 hulls before and after leaching for 6 months in deaerated NaOH solution.

Despite the good corrosion resistance of Zircaloy in reactor, radiation induces defects in the matrix such as dislocation loops (see Figure 5), which could lower the corrosion resistance of the metal in disposal conditions. Optical observations confirmed radiation-induced defects as potential pathways for ^{14}C release, which could explain the higher corrosion rates measured for irradiated Zr-4 against preoxidized Zr-4 (see Figure 10). Additional Raman characterizations revealed band defects around 710 cm^{-1} for irradiated Zr-4 and M5^{TM} hulls before and after leaching in NaOH solution for 6 months (see Figure 11). The intensity of these defects band may vary along with the irradiation damage, but also with the orientation of the zirconia grains. This defect band was attributed to oxygen vacancies.

Understanding Zircaloy Behavior for Use in Performance Assessments

This study gives an overview on ^{14}C released from Zircaloy cladding materials in alkaline media representative of repository conditions. The main conclusions are as follows:

- The ^{14}C inventory was determined both experimentally and by modeling; there was good consistency between the respective results.

- N content was determined experimentally with a concentration in the order of 20–30 ppm.

- The corrosion rates of unirradiated and irradiated Zircaloys were estimated by using several methods (hydrogen measurements, electrochemistry, fraction of released ^{14}C).

° For irradiated Zircaloys, the corrosion rates seem to be around 1–2 nm/yr on the longer term (experimental time was 6.5 years), but initially higher over the first year (up to 100 nm/yr). The oxide layer seems to lower the corrosion kinetics.

° Radiation induces defects that may reduce the corrosion resistance of Zircaloy in disposal conditions.

° Temperature tends to increase the corrosion kinetics while the Zircaloy type does not seem to influence it.

- The Zircaloy type influences ^{14}C inventory and speciation as shown with the results obtained for Zr-4 and M5^{TM} leached in similar conditions (NaOH pH 12 for 6 months).

° The results show an organic fraction that is larger than the inorganic one.

° The speciation seems to evolve with time, according to the results obtained after 6.5 years on irradiated Zr-2 immersed in NaOH solution at pH 12.

° Carboxylic acids were identified by ion chromatography and oxalate was quantified by AMS.

- It is now believed that the IRF to be considered in performance assessment should be lower than the 20% value commonly used.

- The release mechanisms of ^{14}C need more investigation.

° The congruent release of ^{14}C with the metal corrosion rate has not been confirmed.

° Dissolution of zirconia is extremely low at alkaline pH relevant to repository conditions.

REFERENCES

Bucur C, Fulger M, Florea I, Dobrin R, Diaconescu C, Tudose A, Uta O. 2017. Final report on experimental results on long-term corrosion tests and ^{14}C release assessment, irradiated Zircaloy (D3.16). *CArbon-14 Source Term – CAST*. Available from http://www.projectcast.eu.

Cox B. 1985. Assessment of PWR waterside corrosion models and data. *EPRI Technical Report* NP-4287.

Garzarolli F, Jorde D, Manzel R, Parry GW, Smerd PG. 1980. Review of PWR fuel rod waterside corrosion behavior. *EPRI Technical Report* NP-1472.

Gauld IC, Hermann OW, Westfall RM. 2009. ORIGEN scale system module to calculate fuel depletion, actinide transmutation, fission product buildup and decay, and associated radiation terms. *Oak Ridge National Laboratory* ORNL/TM 2005/39. Version 6, Vol. II, Sect. F7.

Gras JM. 1988. Étude bibliographique de la corrosion généralisée des alliages Zircaloy dans les conditions intéressant le fonctionnement des réacteurs à eau légère. *EDF R&D Technical Report* HT-45 PVD654. March 1988. 150 p. In French.

Gras J-M. 2014. State of the art of ^{14}C in Zircaloy and Zr alloys – ^{14}C release from zirconium alloy hulls (D3.1). *CArbon-14 Source Term – CAST*. Available from http://www.projectcast.eu.

IAEA. 1998. Waterside corrosion of zirconium alloys in nuclear power plants. *IAEA-TECDOC* 996.

Hillner E. 1977. Corrosion of zirconium-base alloys—an overview. Zirconium in the Nuclear Industry, 3rd Int. Symp. *ASTM STP* 633:211–35.

Kato O, Tanabe H, Sakuragi T, Nishimura T, Tateishi T. 2013. Corrosion tests of Zircaloy hull waste to confirm applicability of corrosion model and to evaluate influence factors on corrosion rate under geological disposal conditions. Scientific Basis for Nuclear Waste Management XXXVII, Barcelona, Spain, 29 September–3 October 2013. *Mat. Res. Soc. Symp. Proc.* 1518.

Magnusson A, Stenstrom K, Aronsson PO. 2008. ^{14}C in spent ion exchange resins and process water from nuclear reactors – a method for quantitative determination of organic and inorganic fractions. *Journal of Radioanalytical and Nuclear Chemistry* 275(2):261–73.

ORNL. 2011. SCALE: a comprehensive modeling and simulation suite for nuclear safety analysis and design. *Oak Ridge National Laboratory* ORNL/TM-2005-39. Version 6.

Pelowitz DB. 2011. *MCNPX Users Manual*. Version 2.7.0. LA-CP-11-00438.

Sakuragi T. 2018. Final Report on Zr alloys corrosion studies at RWMC (D3.19). *CArbon-14 Source Term – CAST*. Available from http://www.projectcast.eu.

Tanabe H, Sakuragi T, Miyakawa H, Takahashi R. 2013. Long-term corrosion of Zircaloy hull waste

under geological disposal conditions: Corrosion correlations, factors Influencing corrosion, corrosion test data, and preliminary evaluation. Scientific Basis for Nuclear Waste Management XXXVII, Barcelona, Spain, 29 September–3 October 2013. *Mater. Res. Soc. Symp. Proc.* 1518.

Wieland E, Hummel W. 2010. The speciation of ^{14}C in the cementitious near field of a repository for radioactive waste. *PSI Technical Report* TM-44-10-01.

Wilson WB, Cowell ST, England TR, Hayes AC, Moller P. 2008. *A Manual for CINDER'90.* Version 07.4, Codes and Data. LA-UR-07-8412.

Yamaguchi T, Tanuma S, Yasutomi I, Nakayama T, Tanabe H, Katsurai K, Kawamura W, Maeda K, Kitao H, Saigusa M. 1999. A study on chemical forms and migration behaviour of radionuclides in hull wastes. ICEM 1999, September, Nagoya.

Yamashita Y, Tanabe H, Sakuragi T, Takahashi R, Sasoh M. 2013. ^{14}C release behavior and chemical species from irradiated hull waste under geological disposal conditions. Scientific Basis for Nuclear Waste Management XXXVII, Barcelona, Spain, 29 September–3 October 2013. *Mater. Res. Soc. Symp. Proc.* 1518.